An Intelligent Multimode Voice Communications System for Indoor Communications

Lajos Hanzo, *Senior Member, IEEE*, and Jason P. Woodard

***Abstract*— A novel high-quality, low-complexity dual-rate 4.7 and 6.5 kbits/s algebraic code excited linear predictive codec is proposed for adaptive multi-mode speech communicators, which can drop their source rate and speech quality under network control in order to invoke a more error resilient modem amongst less favorable channel conditions. Source-matched binary Bose-Chaudhuri-Hocquenghem (BCH) codecs combined with unequal protection diversity- and pilot-assisted 16- and 64-level quadrature amplitude modulation (16-QAM, 64-QAM) are employed in order to accommodate both the 4.7 and the 6.5 kbits/s coded speech bits at a signaling rate of 3.1 kBd. Assuming an excess bandwidth of 100%, in a bandwidth of 200 kHz 32 time slots can be created, which allows us to support in excess of 50 users, when employing packet reservation multiple access (PRMA). Good communications quality speech is delivered in an equivalent bandwidth of 4 kHz, if the channel signal-to-noise ratio (SNR) and signal-to-interference ratio (SIR) of the benign indoors cordless channel are in excess of about 15 and 25 dB for the lower and higher speech quality 16-QAM and 64-QAM systems, respectively, and the PRMA time-slots are sufficiently uninterfered due to using time-slot classification algorithms and due to the attenuation of partitioning walls and ceilings.**

I. Introduction

IN RECENT years significant research effort has been devoted to personal communications systems (PCS's) [1] for both indoor and outdoor applications. The highest teletraffic demands are likely to arise in future intelligent office buildings, where the benign picocellular environment ensures that high signal to noise ratios (SNR's) prevail and co-channel interferences are mitigated by the partitioning walls, ceilings, and floors. There is much activity in the field of subsystems, such as low-rate speech and video source coding [2]–[17], channel coding [18]–[19] and unequal source-matched error protection [20], [37], modulation [21]–[36], combined modulation and coding [39], [40], multiple access, networking, etc. However, little attention has been devoted to the integration of existing networks with emerging more intelligent ones, as well as to the integration of subsystems [37], [38], [41], [44]. Hence this treatise is dedicated to a range of subsystem integration issues and will explore the trade-offs associated with using an intelligent multi-mode voice terminal, where the expanded signal constellation is exploited to accommodate a higher-rate, better quality speech stream, when the channel conditions allow.

Manuscript received May 20, 1994; revised February 6, 1995. This work was supported by the SERC, UK, under GR/J46845, and the Department of Education, Northern Ireland.

The authors are with the Department of Electrical and Computer Science, University of Southampton, SO17 1BJ, UK.

IEEE Log Number 9413014.

The near future is likely to witness the emergence of intelligent multi-mode mobile speech communicators [45] that can adapt their parameters to rapidly changing propagation environments and maintain a near-optimum combination of transceiver parameters in various scenarios. Therefore it is beneficial, if the transceiver can drop its speech source rate for example from 6.5 kbits/s to 4.7 kbits/s and invoke 16-level quadrature amplitude modulation (16-QAM) instead of 64-QAM, while maintaining the same bandwidth. A typical such re-configuration scenario will be encountered, for example, when a subscriber leaves a benign indoor pico-cellular system and will be handed over to an outdoor micro-cell. Furthermore, in conjunction with intelligent time-slot quality classification algorithms [42], [43] the higher speech quality, less robust mode of operation can be invoked for low-interference time slots, while more contaminated slots can be used by the more robust, lower speech quality 16-QAM mode.

In this contribution the underlying trade-offs of using such a dual-rate Algebraic Code Excited Linear Predictive (ACELP) speech codec in conjunction with a diversity- and pilot-assisted coherent, reconfigurable, unequal error protection 16-QAM/64-QAM modem are investigated. One of the main objectives of the paper is to investigate the feasibility and assess the potential benefits of such an intelligent system using a specific prototype scheme tailored to the 200 kHz bandwidth of the Pan-European GSM system. Section II briefly describes the re-configurable transceiver scheme, Section III details the proposed dual-rate ACELP codec, followed by a short discussion on bit sensitivity issues in Section V, on modulation aspects in Section VI and on source-matched embedded error protection in Section VII. Packet reservation multiple access lends itself to intelligent time-slot classification algorithms, which are vital in terms of ensuring the required signal to interference ratio (SIR), as highlighted in Section VIII. Finally, before concluding, the system performance is characterized in Section IX.

II. The Transceiver Scheme

The schematic diagram of the proposed reconfigurable transceiver is portrayed in Fig. 1. A Voice Activity Detector (VAD) similar to that of the Pan-European GSM system [52] enables or disables the ACELP encoder [8] and queues the active speech frames in the Packet Reservation Multiple Access (PRMA) [53] slot allocator (SLOT ALLOC) for transmission to the base station (BS). The 4.7 or 6.5 kbits/s (kbps) ACELP coded active speech frames are mapped according to their error

0018–9545/95$04.00 © 1995 IEEE

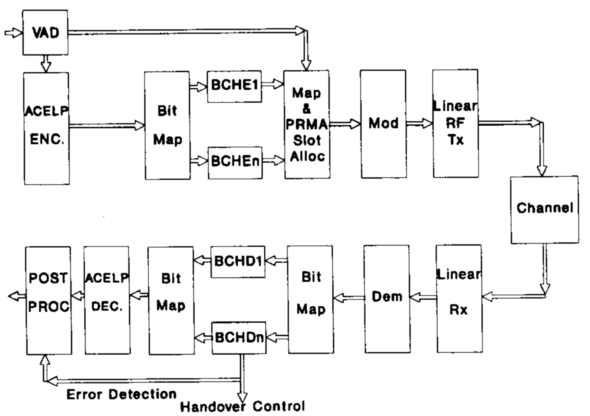

Fig. 1. Transceiver schematic.

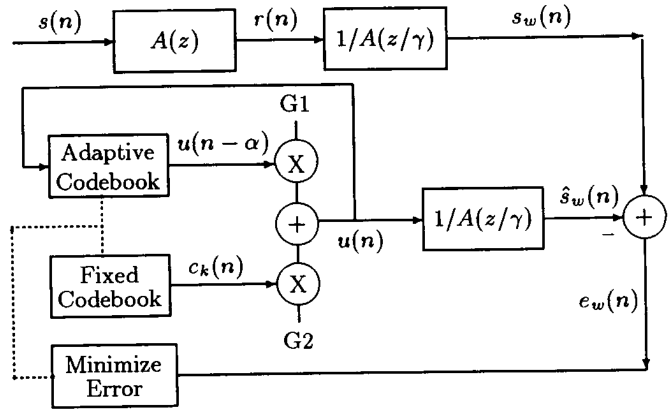

Fig. 2. Speech encoder schematic.

sensitivities to n number of protection classes by the Bit Mapper (BIT MAP), as shown in the figure and source sensitivity-matched binary Bose–Chaudhuri–Hocquenghem (BCH) encoded [18] by the BCHE1 ... BCHEn encoders. "The Map & PRMA Slot Allocator" block converts the binary bit stream to 4- or 6-bit symbols, injects pilot symbols and ramp symbols and allows the packets to contend for a PRMA slot reservation. After BCH encoding the 4.7 and 6.5 kbps speech bits they are mapped to 4- or 6-bit symbols, which are modulating a reconfigurable 16- or 64-level Quadrature Amplitude Modulation (QAM) scheme [36].

We have arranged for the 4.7 kbps/16-QAM and 6.5/64-QAM schemes to have the same signaling rate and bandwidth requirement. Therefore this transmission scheme can provide higher speech quality, if high channel signal-to-noise ratios (SNR) and signal-to-interference ratios (SIR) prevail, while it can be reconfigured under network control to deliver lower, but unimpaired speech quality amongst lower SNR and SIR conditions. Indoors pico-cellular cordless systems have typically friendly, high-SNR and high-SIR nondispersive propagation channels and the partitioning walls also contribute towards attenuating co-channel interferences. Furthermore, the PRMA time-slots can be classified according to the prevailing interference levels evaluated during idle slots and if sufficiently high SIR's prevail, the higher speech quality mode can be invoked, otherwise the more robust, lower speech quality mode of operation must be used.

The modulated signal is then transmitted using the linear radio frequency (RF) transmitter (Tx) over the friendly indoor channel, received by the linear receiver (Rx), demodulated (DEM), and the received speech bits are mapped back to their original bit protection classes by the bit mapper. The n-class BCH decoder BCHD1 ... BCHDn carries out error correction, before ACELP decoding and post processing can take place. Observe that the error detection capability of the strongest BCH decoder, which is more reliable than that of its weaker counterparts, can be used to assist in controlling handovers to a less interfered PRMA time slot on any other available carrier or to activate speech post processing in order to conceal the subjective effects of BCH decoding errors [32]. In contrast to the simple gradually muted previous frame substitution used for example in the Pan-European GSM system [52], we prefer the slightly more sophisticated correlative technique of [32].

III. The Dual-Rate Speech Codec

The schematic of the proposed dual-rate ACELP speech coder is shown in Fig. 2. The transfer function $A(z)$ represents an all zero filter of order ten, which is used to model the short term correlation in the speech signal $s(n)$. The filter coefficients are determined for each 30 ms speech frame by minimizing the variance of the prediction residual $r(n)$, using the autocorrelation method [4]. The coefficients are then converted to Line Spectrum Frequencies (LSF's) [4], which are scalar quantized with a total of 34 bits per frame and transmitted to the decoder. The filter $1/A(z)$, referred to as the synthesis filter, is used in the decoder to produce the reconstructed speech signal from the received excitation signal $u(n)$.

The excitation signal $u(n) = G_1 u(n-\alpha) + G_2 c_k(n)$ seen in Fig. 2 is determined from its G_1-scaled history after adding the G_2-scaled fixed codebook vector $c_k(n)$ for every 5 or 7.5 ms subframe, i.e., four or six times per 30 ms frame. The optimum excitation is chosen to minimize the mean square weighted error E_w over the subframe of $N = 60$ samples for the 4.7 Kbits/s lower speech quality mode and $N = 40$ samples for the 6.5 Kbits/s higher quality mode of operation.

In an optimal codec the fixed codebook index and gain as well as the adaptive codebook parameters would all be jointly optimized in order to minimize E_w. However in practice this is not possible due to the excessive complexity it would entail, and so a suboptimal approach is used. The adaptive codebook parameters are determined first under the assumption of no fixed codebook excitation component, i.e., $G_2 = 0$. It can then be shown [10], [4] that the optimum codebook parameters are the delay α which maximizes the term

$$X = \frac{\left(\sum_{n=0}^{N-1} x(n) y_\alpha(n)\right)^2}{\sum_{n=0}^{N-1} y_\alpha^2(n)} \tag{1}$$

and the gain G_1 given by

$$G_1 = \frac{\sum_{n=0}^{N-1} x(n) y_\alpha(n)}{\sum_{n=0}^{N-1} y_\alpha^2(n)}. \quad (2)$$

Here $x(n) = s_w(n) - \hat{s}_o(n)$ is the weighted speech after removing the memory contribution $\hat{s}_o(n)$ of the weighted synthesis filter $1/A(z/\gamma)$ due to its input in the previous subframe, and $y_\alpha(n) = \Sigma_{i=0}^{n} u(i-\alpha)h(n-i)$ is the convolution of the previous history of $u(i)$ at delay α with the impulse response $h(n)$ of $1/A(z/\gamma)$.

Using 127 legitimate delays, α can be represented using seven bits, while the gain G_1 is quantized with three bits, giving a total of ten bits per subframe for the adaptive codebook information.

A. Fixed Codebook Search

It can be shown that in order to minimize the mean squared weighted error E_w, the codec has to find the optimum gain G_2 for each fixed codebook entry $c_k(n)$ by computing [4]

$$G_2 = \frac{\sum_{n=0}^{N-1} y(n)[c_k(n) * h(n)]}{\sum_{n=0}^{N-1} [c_k(n) * h(n)]^2} = \frac{C_k}{\xi_k} \quad (3)$$

where the shorthand

$$y(n) = s_w(n) - \hat{s}_o(n) - G_1 y_\alpha(n) \quad (4)$$

was used. Here C_k is the correlation between the fixed codebook target $y(n)$ and the filtered innovation sequence $[c_k(n) * h(n)]$, while ξ_k is the energy of the filtered innovation sequence. The gain G_2 is quantized using five bits to yield $\hat{G}_2$ and it can be shown [4] that E_w is minimized by that codebook entry which maximizes the term $T_k = \hat{G}_2(2C_k - \hat{G}_2\xi_k)$.

The CELP codec's complexity arises mainly due to calculating the correlation C_k and energy ξ_k for every codebook entry. Several schemes have been proposed in order to reduce the complexity of the original CELP codec [8], [10], [12], of which here we opted for the highly successful Algebraic CELP (ACELP) structure proposed [5], [6] and refined [7]–[9] by Adoul *et al.* at the University of Sherbrook.

B. Algebraic CELP Codebook Structure

In the ACELP codec structured interlaced permutation codes borrowed from error correction coding [8] define four nonzero pulses 1, −1, 1, −1 in each innovation sequence $c_k(n), n = 0 \cdots N-1$. Each pulse has eight legitimate positions, requiring a total of $3 \times 4 = 12$ bits in order to identify the optimum innovation sequence. The codebook structures are specified in Tables I and II for the 4.7 and 6.5 Kbits/s codecs, respectively. Together with the five bits used to quantize the gain G_2 this gives a total of 17 bits per subframe for the fixed codebook information.

TABLE I
PULSE AMPLITUDES AND POSITIONS FOR 4.7 kbits/s CODEC [4]

Pulse Number	Amplitude	Possible Position
0	+1	0, 8, 16, 24, 32, 40, 48, 56
1	−1	2, 10, 18, 26, 34, 42, 50, 58
2	+1	4, 12, 20, 28, 36, 44, 52
3	−1	6, 14, 22, 30, 38, 46, 54

TABLE II
PULSE AMPLITUDES AND POSITIONS FOR 6.5 kbits/s CODEC

Pulse Number	Amplitude	Possible Position
0	+1	1, 6, 11, 16, 21, 26, 31, 36
1	−1	2, 7, 12, 17, 22, 27, 32, 37
2	+1	3, 8, 13, 18, 23, 28, 33, 38
3	−1	4, 9, 14, 19, 24, 29, 34, 39

TABLE III
NUMBER OF FLOATING POINT OPERATIONS PER SUBFRAME

ACELP Codebook Search	120 000
CELP Codebook Search	31 000 000
Filter and Adaptive Codebook Determination	60 000

The main advantage of the algebraic codebook structure is that it allows the values C_k and ξ_k to be calculated very efficiently [8], [4] using a series of four nested loops and updating a single pulse position at a time. The speech quality can be further improved using 15-bit codebooks and five nested loops, where focused codebook search strategies must be employed [9]–[11].

Table III shows the number of operations used per subframe in determining the fixed codebook parameters for the 4.7 Kbits/s codec. Also shown is the equivalent number for the original nonsparse CELP codebook, and the approximate number of operations required in the rest of the encoding operation as described in this paper. As can be seen from Table III, the codebook search accounts for the majority of the complexity in the coding, and the algebraic codebook structure gives a factor of 258 reduction in terms of complexity. Other advantages of the algebraic codebook structure are that it does not require any codebook storage, and as discussed later it is robust to channel errors.

C. Bit Allocation

As mentioned, the excitation signal $u(n)$ is determined for each 5 or 7.5 ms subsegment of a 30 ms speech frame, depending on the targeted output bit rate, and it is described in terms of the following parameters:

- The adaptive codebook delay α that can take any integer value between 20 and 147 and hence is represented using 7 bits.
- The adaptive codebook gain G_1 which is nonuniformly quantized with 3 bits.
- The index of the optimum fixed codebook entry $c_k(n)$, which is represented with 12 bits.

TABLE IV
DUAL-RATE ACELP BIT ALLOCATION SCHEME

Mode of Operation	4.7 kbits/s	6.5 kbits/s
LSF's	34	34
Fixed C.B. Index k	48 (4×12)	72 (6×12)
Fixed C.B. Gains G_2	20 (4×5)	30 (6×5)
Adaptive C.B. Delays	28 (4×7)	42 (6×7)
Adaptive C.B. Gains G_1	12 (4×3)	18 (6×3)
Total	142	196

TABLE V
ACELP BIT POSITIONS IN THE TRANSMISSION FRAME

Bit Index	Parameter
1 to 34	LSF's
35 to 41	Adaptive Codebook Delay
42 to 44	Adaptive Codebook Gain
45 to 56	Fixed Codebook Index
57	Fixed Codebook Gain Sign
58 to 61	Fixed Codebook Gain

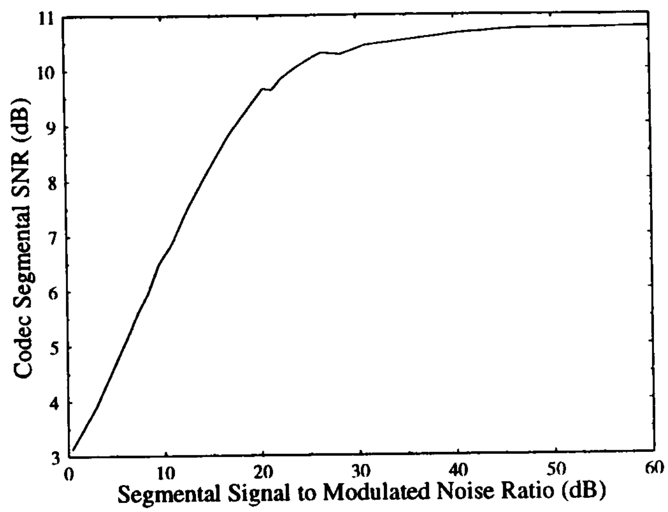

Fig. 3. Performance of 4.7 kbps codec for noisy input signals.

- The fixed codebook gain G_2 which is quantized with a 4 bit logarithmic quantizer and an additional sign bit.

Thus a total of 27 bits are needed to represent the subsegment excitation signal $u(n)$, and for the low-rate mode we have a total of $(34 + 4 \times 27) = 142$ bits per 30 ms frame, or a rate of about 4.7 kbits/s, while in the high rate mode a total of $(34 + 6 \times 27) = 196$ bits per 30 ms frame, yielding a data rate of just over 6.5 kbits/s. These figures are summarized in Table IV and the position of bits in the transmitted frame becomes explicit in Table V.

D. Robustness to Background Noise

An important issue in the design of low bit rate speech codecs is their robustness to background noise. We tested this aspect of our codec's performance using a speech correlated noise source called the modulated noise reference unit, as described in [4]. This method was proposed by Schroeder [56] and standardized by the CCITT. Fig. 3 shows how the segmental SNR of our 4.7 kbps codec varies with the signal to modulated noise ratio. It can be seen that the ACELP codec is not seriously affected by the background noise until the signal to modulated noise ratio falls below about 20 dB.

IV. SPEECH QUALITY

The subjective speech quality produced by the reconfigurable codec is in line with that of other similar schemes at both of its rates and due to the better excitation representation using six rather than four subsegments it sounds more transparent at 6.5 kbps than at 4.7 kbps. As a comparison, the half-rate vector excited linear predictive (VSELP) GSM codec has bit rate of 5.6 kbps, which is between these rates. Having demonstrated the feasibility of reconfigurable low-rate analysis-by-synthesis (ABS) codecs in our future speech research we will attempt to innovate in the area of more flexible embedded codecs covering a wide range of quality and bit rates, as does for example the 16–40 kbps CCITT/ITU G727 predictive waveform codec.

In order to quantify the objective speech degradations inflicted by channel errors, we will employ two widely used objective distance measures, namely, the segmental signal-to-noise ratio (SEGSNR) and the Cepstral Distance (CD) [14]. The former evaluates the SNR in dB for typically 15–30-ms-long speech segments and averages these values in terms of dBs. Since this happens in the logarithmic dB domain, the averaging corresponds to calculating the geometric mean SNR rather than the arithmetic mean SNR. This gives more fair weighting to low-energy unvoiced speech segments during quality evaluation, which would be under-weighted by the conventional SNR in the nonlogarithmic domain. In contrast, the CD quantifies the spectral envelope degradation due to processing and, hence, it is more appropriate for the quality assessment of the coding of spectral parameters. Although to date there is no standardized objective speech quality measure, which would guarantee a direct conversion to the formal five-point subjective Mean Opinion Score (MOS) defined by the CCITT/ITU, the international speech research community is endeavoring to define one [14]–[16]. Although there is a range of computationally more demanding psycho-acoustically motivated measures, such as for example the Bark spectrum [15], the correlation of the simple CD and SEGSNR with the MOS is quoted as 0.63 and 0.77, respectively [15], without specifying the range of bit rates and codecs for which it was evaluated. Similar findings were earlier published for various medium rate codecs for the CD in [14]. Hence in our endeavors we have decided to use a combination of CD and SEGSNR degradations as a relative measure, rather than their actual values.

Let us now briefly focus our attention on the robustness of the ACELP codec against channel errors.

V. ERROR SENSITIVITY ISSUES

The robustness of the short-term spectral LSF's can be improved by exploiting their ordering property [4]. When a nonordered set of LSF's is received, we examine each LSF bit to check whether inverting this bit would eliminate the error. If several alternative bit inversions are found that correct the crossover, then the one that produces LSF's as close as possible to those in the previous frame is used. With this technique we found that when the LSF's are corrupted such that a crossover is encountered, which happens about 30% of the time, the corrupted LSF was correctly identified in more than 90% of the cases, and the corrupted bit was pinpointed about 80% of the time. When this happens, the effect of the bit error is completely removed and so 25% of all LSF errors can be entirely removed by the decoder. When unequal error protection is used, the situation can be further improved because the algorithm will know which bits are more likely to be corrupted, and so can attempt correcting the LSF crossover by inverting these bits first.

The algebraic codebook structure used in our codec is inherently quite robust to channel errors. This is because if one of the codebook index bits is corrupted, the codebook entry selected at the decoder will differ from that used in the encoder only in the position of one of the four nonzero pulses. Thus the corrupted codebook entry will be similar to the original. In conventional CELP codecs when a bit of the codebook index is corrupted, a different codebook address is decoded and the codebook entry used is entirely different from the original, inflicting typically a segmental signal-to-noise ratio (SEGSNR) degradation of about 8 dB. In contrast, our codec exhibits degradation of only about 4 dB when a codebook index bit is corrupted in every frame.

The magnitude of the fixed codebook gain tends to vary quite smoothly from one subframe to the next. If a codebook gain is found which is not in the predicted range, then it is assumed to be corrupted, and replaced with an estimated gain. After careful investigation we implemented a smoother which was able to spot almost 90% of the errors in the most significant bit of the gain level, and reduced the error sensitivity of this bit by a factor of five. The fixed codebook gain sign shows erratic behavior and hence does not lend itself to smoothing. This bit has a high error sensitivity and has to be be well protected by the channel codec.

Seven bits per subframe are used to encode the adaptive codebook delay, and most of these are extremely sensitive to channel errors. An error in one of these bits produces a large SEGSNR degradation not only in the frame in which the error occurred, but also in subsequent frames, and generally it takes more than ten frames before the effect of the error dies out. Therefore these bits should, wherever possible, be strongly protected. The pitch gain is much less smooth than the fixed codebook gain, and hence it is not amenable to smoothing. However its error sensitivity can be reduced by Gray-coding the quantizer levels.

A commonly used approach of quantifying the sensitivity of various coded bits is to consistently invert a given bit with a unity error probability in every frame and evaluate the SEGSNR degradation. The error sensitivity for our 4.7 kbits/s ACELP codec quantified using this method is shown in Fig. 4 for the 34 LSF bits and the 27 first subframe bits. The bit allocation scheme used is shown in Table V. The problem with this approach of quantifying error sensitivity is that it does not take adequate account of the different error propagation properties of different bits. This means that if, instead of corrupting a bit in every frame it is corrupted randomly with some error probability, then the relative sensitivity of different bits will change.

Therefore we propose to employ another error sensitivity measure, which takes account of the error propagation effects. For each bit we find the average SNR degradation due to a single bit error both in the frame in which the error occurs and in consecutive frames. These effects are demonstrated in Fig. 5 for five different bits, each of which belongs to a different parameter, as seen in Table V. Specifically, Bit 2 represents the second bit of the first LSF, which does exhibit some error propagation effects due to the coefficient interpolation between consecutive frames, but the degradation dies down quickly. Bit 40 is one of the adaptive codebook or LTP delay encoding bits and it shows a much more prolonged speech degradation effect over some 15 consecutive frames. Bit 43 is an adaptive codebook or LTP gain bit, which inflicts lower SNR degradations than Bit 40, but has a similarly long decay memory. As mentioned before, the fixed codebook index bits are more robust and hence for example the index Bit 51 is much less sensitive than Bit 40. In contrast, Bit 57, which is the sign bit of the fixed codebook gain has a high and prolonged SNR degradation profile.

Based on these results the total SNR degradation is then found by adding or integrating the degradations caused in the erroneous frame and in all the following frames which are affected by the error. Fig. 6 demonstrates the total SNR degradations evaluated in this way. The graph is significantly different from that in Fig. 4. In particular, the importance of the adaptive codebook delay bits due to their memory propagation becomes more explicit. In contrast, the significance of the LSF's is reduced, since they are recomputed for every new frame and there is only a moderate error propagation due to the interframe interpolation used.

Our final error sensitivity measure is based on the total SNR degradations described above and on a similar measure for the total Cepstral Distance [14] degradation. The two sets of degradation figures are given equal weight and combined to produce an overall sensitivity measure, which is invoked to assign the speech bits to various bit protection classes.

Having characterized the proposed speech codec we now concentrate on the modulation aspects of our transceiver.

VI. Reconfigurable Modulation

The choice of the modulation scheme is a critical issue and it has wide-ranging ramifications as regards to the system's robustness, bandwidth efficiency, power consumption, whether to use an equalizer, etc. In [45] we have shown that due to the fact that Gaussian minimum shift keying (GMSK), $\pi/4$-shifted quaternary phase shift keying ($\pi/4$-DQPSK) and 16-QAM have bandwidth efficiencies of 1.35, 1.64, and 2.4 bps/Hz, respectively, 16-QAM achieves the highest PRMA gain. This is explained by the fact that 16-QAM allows us to generate the highest number of time slots amongst them, given a certain bandwidth, and therefore the statistical multiplexing gain of PRMA can approach the reciprocal of the voice activity

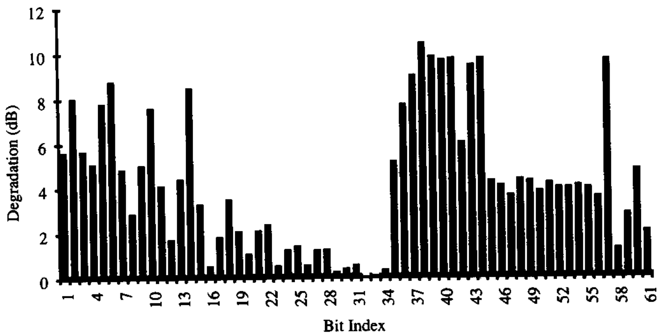

Fig. 4. SEGSNR degradation of the 4.7 kbits/s codec's bits due to 100% bit error rate.

factor. These findings prompted us to opt for multi-level modulation.

In our proposed reconfigurable transceiver the different source rates of the 4.7 and 6.5 kbits/s ACELP codecs will be equalized using a combination of appropriately designed FEC codecs and 4 bits/symbol or 6 bits/symbol modulators. When the channel signal-to-noise ratio (SNR) and signal-to-interference ratio (SIR) are high, as in friendly indoor pico-cells, 64-level Quadrature Amplitude Modulation (64-QAM) is used to convey the 196 bits of the 6.5 kbps ACELP codec. In contrast, for worse channel conditions, for example after a hand-over to an outdoor micro-cell, the 142 bits of the lower quality 4.7 kbps codec are delivered by a more robust 16-QAM modem in the same bandwidth as the 64-QAM scheme.

During the 1980s QAM research was mainly focused at the benign Gaussian telephone line and point-to-point radio applications [21]. However, in recent years a vast body of innovative work has been proposed also for mobile channels [22]–[35]. Although QAM necessitates power-inefficient class A or AB linear amplification [46], [47], for low-power pico- or micro-cellular applications this is not a serious impediment, particularly, if the transceiver's reduced signaling rate allows the receiver to operate without a "power-thirsty" equalizer. The inherent sensitivity of QAM to co-channel interference is partially remedied by the attenuation of the partitioning walls in indoor pico-cells and can be further mitigated using the channel segregation algorithm proposed in [42].

In order to avoid the employment of sensitive linear-phase Nyquist filtering, nonlinear filtering (NLF) joining time-domain signal transitions with a quarter of a period duration raised-cosine segment can be used [36]. In the case of coherent detection it is essential to be able to separate the information modulated on to the in-phase (I) and quadrature-phase (Q) carriers. Coherent detection can be achieved by the help of the Transparent-Tone-In-Band (TTIB) principle proposed by McGeehan and Bateman [49], [50] and studied by Cavers [51], or using Pilot Symbol Assisted Modulation (PSAM) [35], [48].

Noncoherent QAM modems [31] are less complex to implement, but typically require higher SNR and SIR values than their coherent counterparts [36]. Hence in our proposed scheme second-order switched-diversity assisted coherent Pilot

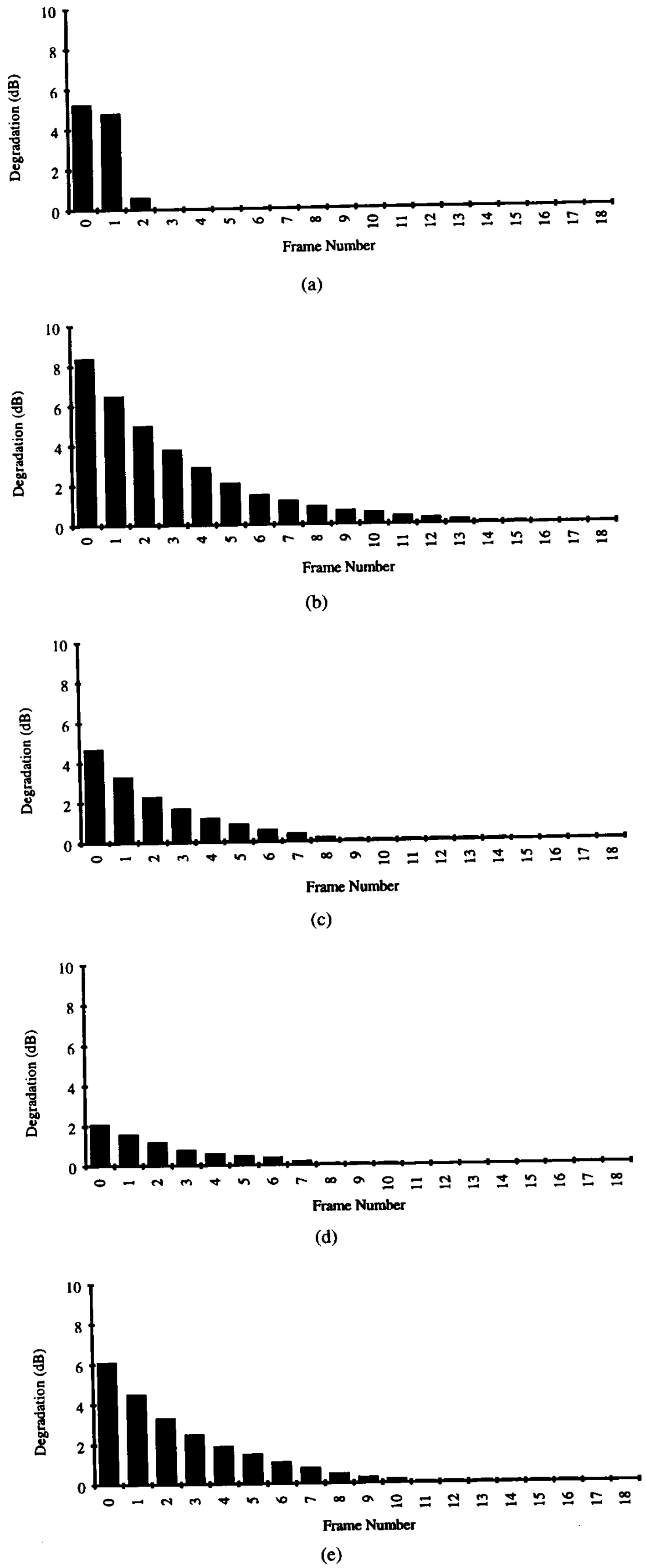

Fig. 5. SNR degradations in consecutive frames for five different bits in the case of the 4.7 kbits/s mode of operation. (a) LSF Bit (Bit 2), (b) STP Delay Bit (Bit 40), (c) LTP Gain Bit (Bit 43), (d) Fixed Codebook Index Bit (Bit 51), (e) Fixed Codebook Gain Sign (Bit 57).

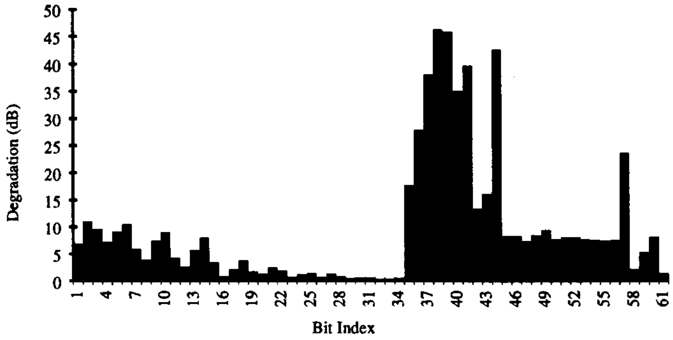

Fig. 6. Total SNR degradation of the 4.7 kbits/s codec due to single errors in various bits.

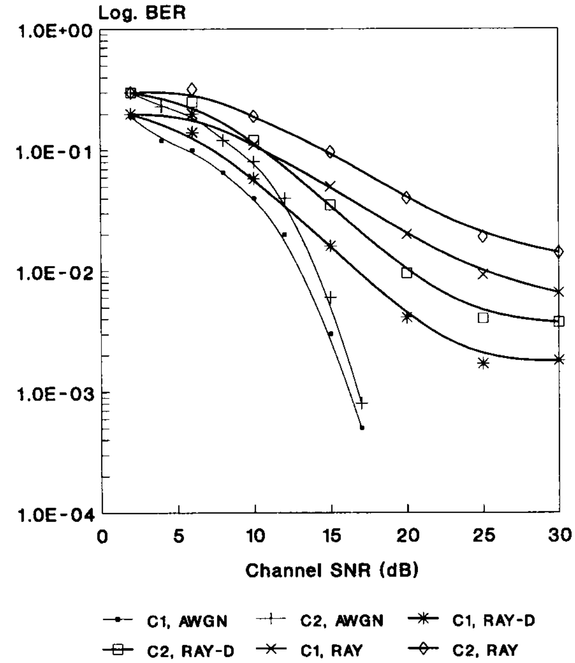

Fig. 7. C1 and C2 BER versus channel SNR performance of 16-QAM using a pilot spacing of $P = 10$ over AWGN and Rayleigh channels at 4 mph, 100 kBd and 1.9 GHz with and without diversity.

Symbol Assisted Modulation (PSAM) using the maximum-minimum-distance square QAM constellation is preferred [36]. For the 16-QAM scheme we have shown [41] that it has two independent subchannels exhibiting different integrities, depending on the position of the bits in a four-bit symbol. On the same note, our 64-QAM modem possesses three different subchannels [44] having different bit error rates. This property naturally lends itself to unequal error protection, if the source sensitivity-matched integrity requirements are satisfied by the QAM subchannel integrities.

Therefore we have evaluated the C1 and C2 bit error rate (BER) versus channel signal-to-noise ratio (SNR) performance of our 16-QAM modem using a pilot spacing of $P = 10$ over both the best-case additive white Gaussian noise (AWGN) channel and over the worst-case Rayleigh-fading channel with and without second-order diversity. The C1 and C2 BER results are shown in Fig. 7 for the experimental conditions characterized by a pedestrian speed of 4 mph, propagation frequency of 1.9 GHz, pilot symbol spacing of $P = 10$ and a signaling rate of 100 kBd. Observe in the figure that over Rayleigh fading channels (RAY) there is an approximately factor three BER difference between the two subchannels both with and without diversity (D). Due to the violent channel phase fluctuations our modem was unable to remove the residual BER floor exhibited at higher channel SNR values, although diversity reception reduced its value by nearly an order of magnitude. The diversity receiver operated on the basis of the minimum channel phase shift within a pilot period, since this condition was found more effective in terms of reducing the BER than the maximum received power condition. Note that in the case of the chosen 100 kBd signaling rate the modulated signal will fit in a bandwidth of 200 kHz, when using a 100% excess bandwidth. Since this coincides with the bandwidth of the Pan-European GSM system [52], we will be able to make direct comparisons in terms of the number of users supported. This will allow us to assess the potential benefits of using multi-mode terminals constituted by third generation system components in terms the increased number of users supported.

How this BER difference between the two subchannels can be exploited in order to provide source-matched FEC protection for the 4.7 kbps ACELP codec will be described in the next section. Following a similar approach for the 6.5 kbps/64-QAM scheme leads to the system proposed as a reconfigurable alternative, which will also be introduced in the next section. Suffice to say here that the BER versus channel SNR performance of this more vulnerable but higher speech quality 64-QAM scheme is portrayed under the same propagation conditions as in the case of the 16-QAM modem in Fig. 8, when using a pilot spacing of $P = 5$. As expected, this diversity and pilot-assisted modem also exhibits a residual BER floor and there is a characteristic BER difference of about a factor of two between the C1 and C2, as well as the C2 and C3 subchannels, respectively. Rather than equalizing these BER differences we will design an unequal error protection scheme for the speech bits, which capitalizes on this property.

VII. Source-Matched Error Protection

A. *Low-Quality Mode*

Recent advances in coded modulation and bandwidth efficient transmission published [39], [40] provide a plethora of attractive transceiver schemes for fading mobile channels. However, for the ACELP speech codec source sensitivity-matched unequal error protection has to be used. Hagenauer introduced rate compatible punctured convolutional (RCPC) codecs [19] in order to perfectly match the FEC power to the sensitivity of the source bits. In order to provide coded modulation schemes having un-equal source-sensitivity matched error protection similarly to our approach in [41] and [44], Wei [20] suggested a range of non-uniformly spaced phasor constellations. Another method proposed by Wei [20] was to deploy a number of independent coded modulation

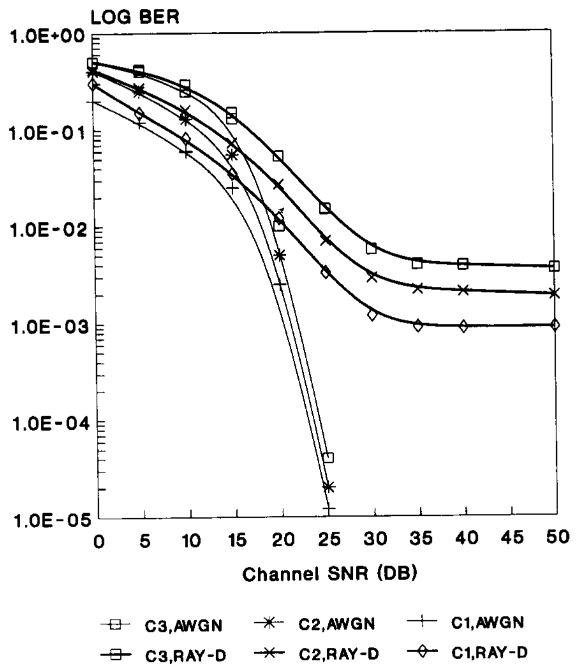

Fig. 8. C1, C2, and C3 BER versus channel SNR performance of 64-QAM using a pilot spacing of $P = 5$ over AWGN and Rayleigh channels with diversity at 4 mph, 100 kBd, and 1.9 GHz.

schemes having different grades of protection and multiplex the sequences for transmission.

In this section we will exploit the subchannel integrity differences highlighted in the previous section in Figs. 7 and 8, and protect these subchannels with source-sensitivity matched binary Bose-Chaudhuri-Hocquenghem (BCH) FEC codecs. Both convolutional and block codes can be successfully employed over bursty mobile channels [18] and convolutional codes have found favor in systems, such as the GSM system, where the complexity of soft-decisions is acceptable [52]. Their disadvantage is that they cannot reliably detect decoding errors and hence they are typically combined with an external error detecting block code, as in the GSM system. In contrast, powerful block codes have an inherent reliable error detection capability in addition to their error correction capability, which can be exploited to invoke error concealment or to initiate handovers, when the average bit error rate is high, as portrayed in Fig. 1.

The error sensitivity of the 4.7 kbps ACELP source bits was evaluated in Figs. 4 and 6, but the number of bit protection classes n still remains to be resolved. Intuitively, one would expect that the more closely the FEC protection power is matched to the source sensitivity, the higher the robustness. In order to limit the system's complexity and the variety of candidate schemes, in the case of the 4.7 kbits/s ACELP codec we have experimented with a full-class BCH codec, a twin-class and a quad-class scheme, while maintaining the same coding rate.

For the full-class system we decided to use the approximately half-rate BCH (127, 71, 9) codec in both subchannels, which can correct 9 errors in each 127-bits block, while encoding 71 primary information bits. The coding rate is $R = 71/127 \approx 0.56$ and the error correction capability is about 7%. Observe that this code curtails BCD decoding error propagation across the speech frame boundaries by encoding each 142-bit speech frame using two BCH (127, 71, 9) frames, although even a single BCH decoding error will inflict prolonged speech impairments, as portrayed in Fig. 5.

In order to design the twin-class system, initially we divided the ACELP bits into two sensitivity classes, Class One and Class Two, which are distinct from the C1 and C2 16-QAM subchannels. Both Class One and Two contained 71 bits. Then we evaluated the SEGSNR degradation inflicted by certain fixed channel BER's maintained in each of the classes using randomly distributed errors, while keeping bits of the other class intact. These experiments suggested that an approximately five times lower BER was required by the more sensitive Class One bits in order restrict the SEGSNR degradations to similar values to those of the Class Two bits.

Recall from Fig. 7 that the 16-QAM C1 and C2 subchannel BER ratio was limited to about a factor of three. Hence we decided to employ a stronger FEC code to protect the Class One ACELP bits transmitted over the 16-QAM C1 subchannel than for the Class Two speech bits conveyed over the lower integrity C2 16-QAM subchannel, while maintaining the same number of BCH-coded bits in both subchannels. However, the increased number of redundancy bits of stronger BCH codecs requires that a higher number of sensitive ACELP bits are directed to the lower integrity C2 16-QAM subchannel, whose coding power must be concurrently reduced in order to accommodate more source bits. This nonlinear optimization problem can only be solved experimentally, assuming a certain subdivision of the source bits, which would match a given pair of BCH codecs.

Based on our previous findings as regards to the C1 and C2 16-QAM BERs and taking account of the practical FEC correcting power limitations we then decided to increase the C1–C2 16-QAM subchannel BER ratio from about three by about a factor of two so that the Class One ACELP bits were guaranteed a BER advantage of about a factor of six over the more robust Class Two bits. After some experimentation we found that the BCH (127, 57, 11) and BCH (127, 85, 6) codes employed in the C1 and C2 16-QAM subchannels provided the required integrity. The SEGSNR degradation caused by a certain fixed BER assuming randomly distributed errors is portrayed in Fig. 9 for both the full-class and the above twin-class system, where the number of ACELP bits in the protection Classes One and Two is 57 and 85, respectively. Note that the coding rate of this system is the same as that of the full-class scheme and each 142-bit ACELP frame is encoded by two BCH codewords. This yields again $2 \cdot 127 = 254$ encoded bits and curtails BCH decoding error propagation across speech segments, although the speech codec's memory will still be corrupted and hence will prolong speech impairments. The FEC-coded bit rate became ≈ 8.5 kbps.

The BER versus channel SNR performance of our twin-class C1, BCH (127, 57, 11)-protected and C2, BCH (127, 85, 6)-protected diversity-assisted 16-QAM modem is shown in Fig. 10 along with the curves C1, Ray-D and C2, Ray-D

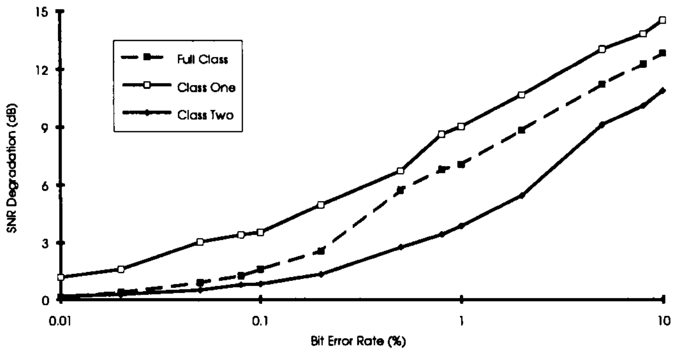

Fig. 9. SEGSNR degradation versus bit error rate for the 4.7 kbps ACELP codec when mapping 71 ACELP bits to both classes one and two in the full-class system and 57 as well as 85 bits to classes one and two in the twin-class scheme, respectively.

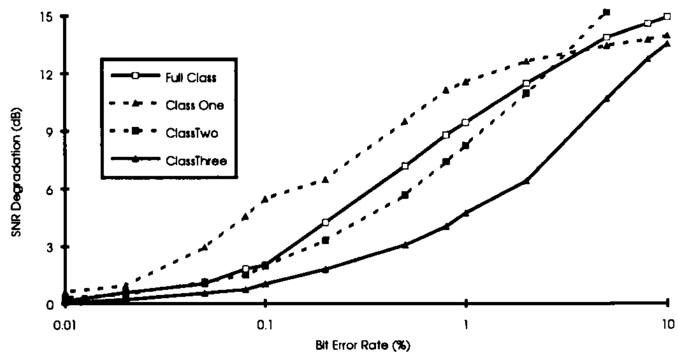

Fig. 11. SEGSNR degradation versus bit error rate for the 6.5 kbps ACELP codec when using either the full-class scheme or mapping 49, 63, and 84 ACELP bits to classes one, two, and three in the triple-class scheme, respectively.

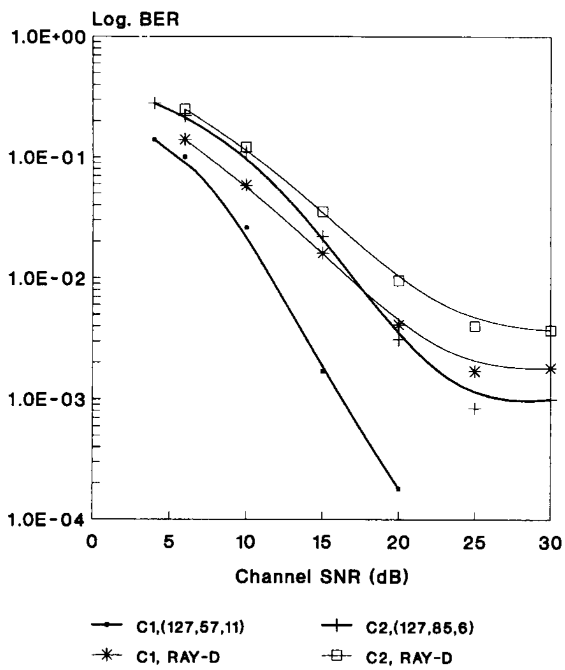

Fig. 10. C1 and C2 BER versus channel SNR performance of 16-QAM using a pilot spacing of $P = 10$ over Rayleigh channels at 4 mph, 100 kBd and 1.9 GHz with diversity and FEC coding.

characteristic of the diversity-assisted no-FEC Rayleigh-fading scenarios, which are repeated here from Fig. 7 for ease of reference. Observe that between the SNR values of 15–20 dB there is about an order of magnitude BER difference between the FEC-coded subchannels, as required by the 4.7 kbps speech codec.

With the incentive of perfectly matching the FEC coding power and the number of bits in the distinct protection classes to the ACELP source sensitivity requirements we also designed a quad-class system, while maintaining the same coding rate. We used the BCH (63, 24, 7), BCH (63, 30, 6), BCH (63, 36, 5) and BCH (63, 51, 2) codes and transmitted the most sensitive bits over the C1 16-QAM subchannel using the two strongest codes and relegated the rest of them to the C2 subchannel, protected by the two weaker codes.

The PRMA control header [53], [54] was for all three schemes allocated a BCH (63, 24, 7) code and hence the total PRMA framelength became 317 bits, representing 30 ms speech and yielding a bit rate of $\approx$ 10.57 kbps. The 317 bits give 80 16-QAM symbols and 9 pilot symbols as well as $2 + 2 = 4$ ramp symbols, resulting in a PRMA framelength of 93 symbols per 30 ms slot. Hence the signaling rate becomes 3.1 kBd. Using a PRMA bandwidth of 200 kHz, similarly to the Pan-European GSM system and a filtering excess bandwidth of 100% allowed us to accommodate 100 kBd/3.1 kBd $\approx$ 32 PRMA slots.

B. High-Quality Mode

Following the approach proposed in the previous subsection we designed a triple-class source-matched protection scheme for the 6.5 kbps ACELP codec. The C1, C2, and C3 64-QAM subchannel performance was characterized by Fig. 8, when using second-order switched-diversity and pilot-symbol assisted coherent square-constellation 64-QAM [36] amongst our previously stipulated propagation conditions with a pilot-spacing of $P = 5$. The BER ratio of the C1, C2 and C3 subchannels was about 1 : 2 : 4.

The SEGSNR degradation versus channel BER performance of the 6.5 kbits/s higher-quality mode is portrayed in Fig. 11, when using randomly distributed bit errors and assigning 49, 63, and 84 bits to the three sensitivity classes. For reference we have also included the sensitivity curve for the full-class codec. As we have seen for the lower-quality 16-QAM mode of operation, the modem subchannel BER differences had to be further emphasized using stronger FEC codes for the transmission of the more vulnerable speech bits.

The appropriate source sensitivity-matched codes for the C1, C2, and C3 subchannels were found to be the shortened 13-error correcting BCH 13 = BCH (126, 49, 13), the 10-error correcting BCH 10 = BCH (126, 63, 10), and the 6-error correcting BCH 6 = BCH (126, 84, 6) codes, while the packet header was allocated again a BCH (63, 24, 7) code. The corresponding BER versus channel SNR curves are presented for our standard propagation conditions in Fig. 12, where the nonprotected diversity-assisted Rayleigh BER curves are

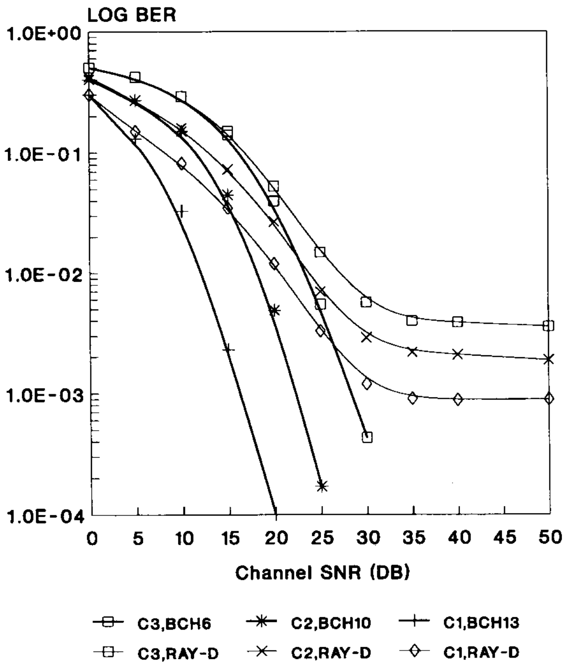

Fig. 12. C1, C2, and C3 BER versus channel SNR performance of PSAM-assisted 64-QAM using a pilot spacing of $P = 5$ over Rayleigh channels at 4 mph, 100 kBd and 1.9 GHz with diversity and FEC coding.

also repeated for convenience. These codes allowed us to satisfy both the integrity and the bit packing requirements, while curtailing bit error propagation across speech frame boundaries.

The total number of BCH -coded bits becomes $3 \times 126 + 63 = 441/30$ ms, yielding a bit rate of 14.7 kbps. The resulting 74 64-QAM symbols are amalgamated with 15 pilot and 4 ramp symbols, giving 93 symbols/30 ms, which is equivalent to a signaling rate of 3.1 kBd, as in the case of the low-quality mode of operation. Again, 32 PRMA slots can be created, as for the low-quality system, accommodating more than 50 speech users in a bandwidth of 200 kHz and yielding a speech user bandwidth of about 4 kHz, while maintaining a packet dropping probability of about 1%.

VIII. Voice Activity Detection and Packet Reservation Multiple Access

In the modulation section we have noted that multi-level modulation conveniently increases the number of time slots, which in turn results in higher PRMA statistical multiplexing gain than in the case of binary modulation. The operation of the voice activity detector (VAD) [52], [55] has a profound effect as regards to the overall subjective speech quality. The fundamental design problem is that on one hand the VAD must respond to an active speech spurt almost instantaneously in order to queue the active speech packet for transmission to the BS and hence minimize front-end speech spurt clipping. On the other hand, it has to have a low false triggering rate even in the presence of high level acoustic background noise, which imposes a taxing design problem, since the input signal's statistics must be observed for some length of time in order to differentiate between speech and noise reliably. In our GSM-like VAD [52] a combination of signal power, stationarity and spectral envelope based decisions is carried out before speech is deemed to be present. In order to prevent prematurely curtailing active spurts during low-energy voiced sounds also a so-called hangover switch-off delay of one speech frame length or 30 ms was imposed. The VAD that we proposed in [55] had a lower complexity and faster reaction time than the GSM VAD, but it was designed for conventional satellite-based telephone systems, where the acoustic background noise is typically more benign than in mobile environments. The GSM VAD was designed and extensively tested by an international expert body and for further details on it the interested reader is referred to [52].

PRMA was designed for conveying speech signals on a flexible demand basis via time division multiple access (TDMA) systems [53], [54]. In our system a voice activity detector (VAD) similar to that of the GSM system [52] queues the active speech spurts to contend for an up-link TDMA time-slot for transmission to the BS. Inactive users' TDMA time slots are offered by the BS to other users, who become active and are allowed to contend for the unused time slots with a given permission probability P_{perm}. In order to prevent colliding users from consistently colliding in their further attempts to attain a time-slot reservation we have $P_{\text{perm}} < 1$. If several users attempt to transmit their packets in a previously free slot, they collide and none of them will attain a reservation. In contrast, if the BS receives a packet from a single user, or succeeds to decode an uncorrupted packet despite of a simultaneous transmission attempt, then a reservation is granted. When the system is heavily loaded, the collision probability is increased and hence a speech packet might have to keep contending in vain, until its life span expires due to the imminence of a new speech packet's arrival after 30 ms. In this case the speech packet must be dropped, but the packet dropping probability must be kept below 1%. Since packet dropping is typically encountered at the beginning of a new speech spurt, its subjective effects are perceptually insignificant.

Our transceiver used a signaling rate of 100 kBd, in order for the modulated signal to fit in a 200 kHz GSM channel slot, when using a QAM excess bandwidth of 100%. The number of time-slots created became TRUNC (100 kBd/3.1 kBd) = 32, where TRUNC represents truncation to the nearest integer, while the slot duration was 30 ms/32 = 0.9375 ms. One of the PRMA users was transmitting speech signals recorded during a telephone conversation, while all the other users generated negative exponentially distributed speech spurts and speech gaps with mean durations of 1 and 1.35 s. These PRMA parameters are summarized in Table VI.

In conventional Time Division Multiple Access (TDMA) systems the reception quality degrades due to speech impairments caused by call blocking, hand-over failures and corrupted speech frames due to noise, as well as co- and adjacent-channel interference. In PRMA systems calls are not blocked due to the lack of an idle time-slot. Instead, the number of contending users is increased by one, slightly inconveniencing all other users, but the packet dropping probability

TABLE VI
SUMMARY OF PRMA PARAMETERS

PRMA parameters	
Channel rate	100 kBd
Source rate	3.1 kBd
Frame duration	30 ms
No. of slots	32
Slot duration	0.9375 ms
Header length	63 bits
Maximum packet delay	30 ms
Permission probability	0.2

is increased only gracefully. Hand-overs will be performed in the form of contention for an un-interfered idle time slot provided by the specific BS offering the highest signal quality amongst the potential target BSs.

If the link degrades before the next active spurt is due for transmission, the subsequent contention phase is likely to establish a link with another BS. Hence this process will have a favorable effect on the channel's quality, effectively simulating a diversity system having independent fading channels and limiting the time spent by the MS in deep fades, thereby avoiding channels with high noise or interference.

This attractive PRMA feature can be capitalized upon in order to train the channel segregation scheme proposed in [42]. Accordingly, each BS evaluates and ranks the quality of its idle physical channels constituted by the unused time slots on a frame-by-frame basis and identifies a certain number of slots, N, with the highest quality. i.e., lowest noise and interference. The slot-status is broadcast by the BS to the portable stations (PS's) and top-grade slots are contended for using the less robust, high speech quality 64-QAM mode of operation, while lower quality slots attract contention using the lower speech quality, more robust 16-QAM mode of operation. Lastly, the lowest quality idle slots currently impaired by noise and interference can be temporarily disabled. When using this algorithm, the BS is likely to receive a signal benefiting from high SNR and SIR values, minimizing the probability of packet corruption due to interference and noise. However, due to disabling the lowest-SNR and -SIR slots the probability of packet dropping due to collision is increased, reducing the number of users supported. When a successful, uncontended reservation takes place using the high speech quality 64-QAM mode, the BS promotes the highest quality second-grade time slot to the set of top-grade slots, unless its quality is unacceptably low. Similarly, the best temporarily disabled slot can be promoted to the second-grade set in order to minimize the collision probability, if its quality is adequate for 16-QAM transmissions.

With the system elements described we now focus our attention on the the performance of the reconfigurable transceiver proposed.

IX. SYSTEM PERFORMANCE AND CONCLUSIONS

The number of speech users supported by the 32-slot PRMA system becomes explicit from Fig. 13, where the packet dropping probability versus number of users is displayed. Observe

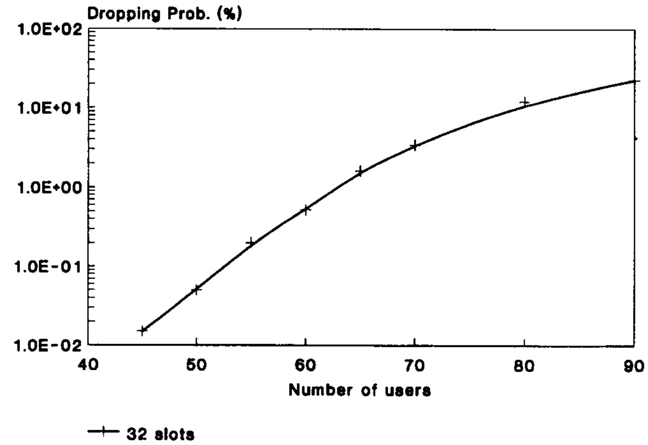

Fig. 13. Packet dropping probability versus number of users for 32-slot PRMA.

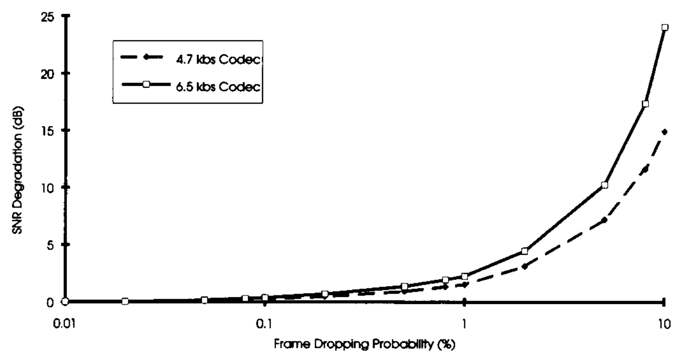

Fig. 14. Speech SEGSNR degradation versus packet dropping probability for the 4.7 and 6.5 kbits/s ACELP codecs.

that more than 55 users can be served with a dropping probability below 1%. The effect of various packet dropping probabilities on the objective speech SEGSNR quality measure is portrayed Fig. 14 for both the 4.7 kbps and the 6.5 kbps mode of operation. This figure implies that packet dropping due to PRMA collisions is more detrimental in case of the higher quality 6.5 kbps codec, since it has an originally higher SEGSNR. In order to restrict the subjective effects of PRMA-imposed packet dropping, according to Fig. 13 the number of users must be below 60. However, in generating Fig. 14, packets were dropped on a random basis and the same 1% dropping probability associated with initial clipping only imposes much less subjective annoyance or speech quality penalty than intra-spurt packet loss would. As a comparative basis it is worth noting that the 8 kbps CCITT/ITU ACELP candidate codec's target was to inflict less than 0.5 Mean Opinion Score (MOS) degradation in case of a speech frame error rate of 3% [9].

The overall SEGSNR versus channel SNR performance of the proposed speech transceiver is displayed in Fig. 15 for the various systems studied, where no packets were dropped, as in a TDMA system supporting 32 subscribers. Observe that the source sensitivity-matched twin-class and quad-class 4.7 kbps ACELP-based 16-QAM systems have a virtually

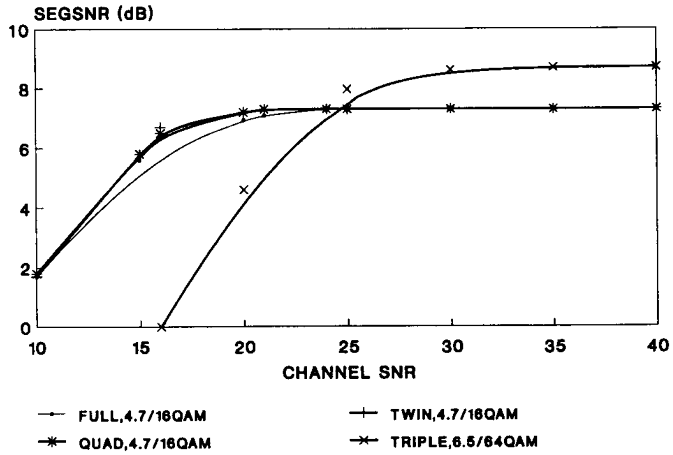

Fig. 15. SEGSNR versus channel SNR performance of the proposed 100 kBd transceiver using 32-slot TDMA.

TABLE VII
TRANSCEIVER PARAMETERS

Parameter	Low/High Quality Mode
Speech Codec	4.7/6.5 kbps ACELP
FEC	Twin-/Triple-class Binary BCH
FEC-coded Rate	8.5/12.6 kbps
Modulation	Square 16-QAM/64-QAM
Demodulation	Coherent Diversity PSAM-assisted
Equalizer	No
User's Signaling Rate	3.1 kBd
VAD	GSM-like [52]
Multiple Acess	32-slot PRMA
Speech Frame Length	30 ms
Slot Length	0.9375 ms
Channel Rate	100 kBd
System Bandwidth	200 kHz
No. of Users	>50
Equivalent User Bandwidth	4 kHz
Min. Channel SNR	15/25 dB

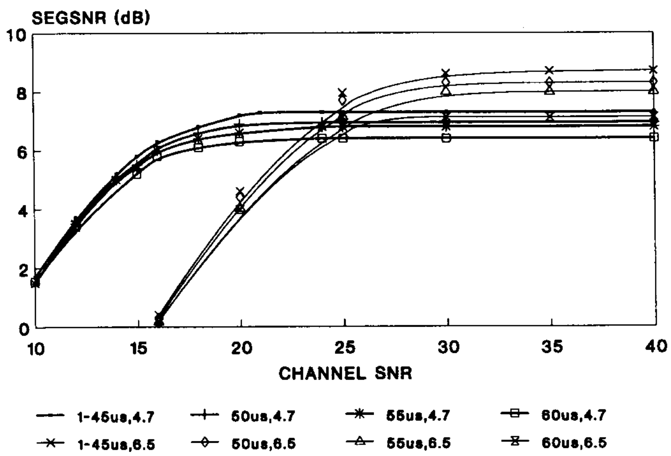

Fig. 16. SEGSNR versus channel SNR performance of the reconfigurable 100 kBd transceiver using 32-slot PRMA for different number of conversations.

identical performance, suggesting that using two appropriately matched protection classes provides adequate system performance, while maintaining a lower complexity than the quad-class scheme. The full-class 4.7 kbps/16-QAM system was outperformed by both source-matched schemes by about 4 dB in terms of channel SNR, the latter systems requiring an SNR in excess of about 15 dB for nearly unimpaired speech quality over our pedestrian Rayleigh-fading channel. When the channel SNR was in excess of about 25 dB, the 6.5 kbps/64-QAM system outperformed the 4.7/16-QAM scheme in terms of both objective and subjective speech quality. When the proportion of corrupted speech frames due to channel-induced impairments and due to random packet dropping as in Fig. 14 was identical, similar objective and subjective speech degradations were experienced. Furthermore, at around a 25 dB channel SNR, where the 16-QAM and 64-QAM SEGSNR curves cross each other in Fig. 15 it is preferable to use the inherently lower quality but unimpaired mode of operation. When supporting more than 32 users, as in our PRMA-assisted system, speech quality degradation is experienced due to packet corruption caused by channel impairments and packet dropping caused by collisions. These impairments yield different subjective perceptual degradation, which we will attempt to compare in terms of the objective SEGSNR degradation. Quantifying these speech imperfections in relative terms in contrast to each other will allow system designers to adequately split the tolerable overall speech degradation between packet dropping and packet corruption. The corresponding SEGSNR versus channel SNR curves for the twin-class 4.7 kbps/16-QAM and the triple-class 6.5 kbps/64-QAM operational modes are shown in Fig. 16 for various number of users between one and 60. Observe that the rate of change of the SEGSNR curves is more dramatic due to packet corruption caused by low-SNR channel conditions than due to increasing the number of users.

As long as the number of users does not significantly exceed 50, the subjective effects of PRMA packet dropping show an even more benign speech quality penalty than that suggested by the objective SEGSNR degradation, because frames are typically dropped at the beginning of a speech spurt due to a failed contention.

In conclusion, our reconfigurable transceiver has a single-user rate of 3.1 kBd, and can accommodate 32 PRMA slots at a PRMA rate of 100 kBd in a bandwidth of 200 kHz. The number of users supported is in excess of 50 and the minimum channel SNR for the lower speech quality mode is about 15 dB, while for the higher quality mode about 25 dB. The number of time slots can be further increased to 42, when opting for a modulation access bandwidth of 50%, accommodating a signaling rate of 133 kBd within the 200 kHz system bandwidth. This will inflict a slight bit error rate penalty, but pay dividends in terms of increasing the number of PRMA users by about 20. The parameters of the proposed transceiver are summarized in Table VII. In order to minimize packet corruption due to interference, the employment of a time-slot quality ranking algorithm is essential for invoking the appropriate mode of operation. When serving 50 users the effective user bandwidth becomes 4 kHz which guarantees the convenience of wireless digital speech communication in a bandwidth similar to conventional analogue telephone channels.

Our future work in the field of speech coding and modulation will be targeted at creating a more finely graded set of reconfigurable subsystems in terms of speech quality, transmission rate, and robustness. These new subsystems will enable us to match the mode of operation more closely with the prevailing channel quality. Further algorithmic research is required in order to define specific control algorithms to accommodate various operating conditions, in particular in the area of appropriate time-slot classification algorithms to invoke the best matching mode of operation and find the best compromise between packet dropping due to collision and packet corruption due to channel impairments.

ACKNOWLEDGMENT

The helpful suggestions of the anonymous reviewers are gratefully acknowledged.

REFERENCES

[1] *IEEE Commun. Mag.*, vol. 30, no. 12, pp. 30–133, Dec. 1992.
[2] *IEEE J. Select. Areas Commun.*, vol. 10, no. 5, pp. 793–976, June 1992.
[3] N. Jayant and R. V. Cox, "Speech codecs for personal communications," *IEEE Commun. Mag.*, vol. 31, no. 11, Nov. 1993.
[4] R. A. Salami, L. Hanzo *et al.*, "Speech Coding," in *Mobile Radio Communications,* R. Steele, Ed. London: Pentech, 1992, ch. 3, pp. 186–346.
[5] J.-P. Adoul and C. Lamblin, "A comparison of some algebraic structures for CELP coding of speech," in *Proc. ICASSP'87,* pp. 1953–1956.
[6] J.-P. Adoul *et al.*, "Fast CELP coding based on algebraic codes," in *Proc. ICASSP'87,* pp. 1957–1960.
[7] C. Lamblin, J.-P. Adoul, *et al.*, "Fast CELP coding based on the Barnes-Wall lattice in 16 dimension," in *Proc. ICASSP'89,* Glasgow, UK, pp. 61–64.
[8] H. C. Laflamme, J.-P. Adoul, H. Y. Su, and S. Morissette, "On reducing the complexity of codebook search in CELP through the use of algebraic codes," in *Proc. ICASSP 1990,* Albuquerque, NM, 1990, pp. 177–180.
[9] R. A. Salami, C. Laflamme, J.-P. Adoul, and D. Massaloux, "A toll quality 8 Kb/s speech codec for the personal communications system (PCS)," *IEEE Trans. Veh. Technol.*, vol. 43, no. 3, pp. 808–816, Aug. 1994.
[10] R. A. Salami, "Binary pulse excitation: A novel approach to low complexity CELP coding," in *Advances in Speech Coding,* B. S. Atal *et al.*, Eds. Norwell, MA: Kluwer, 1991.
[11] R. A. Salami, C. Laflamme, and J. P. Adoul, "ACELP speech coding at 8 kbit/s with a 10 ms frame: A candidate for CCITT standardization," in *Proc. IEEE Workshop on Speech Coding for Telecommun.*, Sainte-Adele, Quebec, Canada, Oct. 13–15, 1993, pp. 23–24.
[12] I. A. Gerson and M. A. Jasiuk, "Vector sum excitation linear prediction (VSELP) speech coding at 8 kbps," in *Proc. ICASSP'90,* Albuquerque, NM, Apr. 3–6, 1990, pp. 461–464.
[13] J.-P. Adoul *et al.*, "Fast CELP coding based on algebraic codes," in *Proc. ICASSP'87,* 1987, pp. 1957–1960.
[14] N. M. Honda and N. Itoh, "Speech quality assesment methods for speech-coding systems," *IEEE Commun. Mag.*, pp. 26–33, Oct. 1984.
[15] S. Wang, A. Sekey, and A. Gersho, "An objective measure for predicting subjective quality of speech coders," *IEEE J. Select. Areas Commun.*, vol. 10, no. 5, pp. 819–829, June 1992.
[16] N. B. Seitz, S. Wolf, S. Voran, and R. Bloomfield, "User-oriented measures of telecommunications quality," *IEEE Commun. Mag.*, pp. 57–66, Jan. 1994.
[17] R. V. Cox, W. B. Kleijn, and P. Kroon, "Robust CELP coders for noisy backgrounds and noisy channels," in *Proc. ICASSP 1989,* 1989, pp. 739–742.
[18] K. H. H. Wong and L. Hanzo, "Channel coding," in *Mobile Radio Communications,* R. Steele, Ed. London: Pentech Press, 1992, ch. 4, pp. 347–488.
[19] J. Hagenauer, "Rate-compatible punctured convolutional codes (RCPC) and their applications," *IEEE Trans. Commun.*, vol. 36, no. 4, pp. 389–400, Apr. 1988.
[20] L. F. Wei, "Coded modulation with unequal error protection," *IEEE Trans. Commun.*, vol. 41, no. 10, pp. 1439–1450, Oct. 1993.
[21] G. D. Forney *et al.*, "Efficient modulation for band-limited channels," *IEEE J. Select. Areas Commun.*, vol. SAC-2, no. 5, pp. 632–647, Sept. 1984.
[22] K. Feher, "Modems for emerging digital cellular mobile systems," *IEEE Trans. Veh. Technol,* vol. 40, no. 2, pp. 355–365, May 1991.
[23] M. Iida and K. Sakniwa, "Frequency selective compensation technology of digital 16-QAM for microcellular mobile radio communication systems," in *Proc. VTC'92,* Denver, CO, pp. 662–665.
[24] R. J. Castle and J. P. McGeehan, "A multilevel differential modem for narrowband fading channels," in *Proc. VTC'92,* Denver, CO, pp. 104–109.
[25] D. J. Purle, A. R. Nix, M. A. Beach, and J. P. McGeehan; "A preliminary performance evaluation of a linear frequency hopped modem," in *Proc. VTC'92,* Denver, CO, pp. 120–124.
[26] Y. Kamio and S. Sampei, "Performance of reduced complexity DFE using bidirectional equalizing in land mobile communications," in *Proc. VTC'92,* Denver, CO, pp. 372–376.
[27] T. Nagayasu, S. Sampei, and Y. Kamio, "Performance of 16-QAM with decision feedback equalizer using interpolation for land mobile communications," in *Proc. VTC'92,* Denver, CO, pp. 384–387.
[28] E. Malkamaki, "Binary and multilevel offset QAM, spectrum efficient modulation schemes for personal communications," in *Proc. VTC'92,* Denver, CO, pp. 325–378.
[29] Z. Wan and K. Feher, "Improved efficiency CDMA by constant envelope SQAM," in *Proc. VTC'92,* Denver, CO, pp. 51–55.
[30] H. Sasaoka, "Block coded 16-QAM/TDMA cellular radio system using cyclical slow frequency hopping," in *Proc. VTC'92,* Denver, CO, pp. 405–408.
[31] W. T. Webb, L. Hanzo, and R. Steele, "Bandwidth-efficient QAM schemes for rayleigh-fading channels," *IEE Proc.*, vol. 138, no. 3, pp. 169–175, June 1991.
[32] L. Hanzo, R. Steele, and P. M. Fortune, "A subband coding, BCH coding and 16-QAM system for mobile radio speech communications," *IEEE Trans. Veh. Technol.*, vol. 39, no. 4, pp. 327–339, Nov. 1990.
[33] T. Sunaga and S. Sampei, "Performance of multi-level QAM with post-detection maximal ratio combining space diversity for digital land-mobile radio communications," *IEEE Trans. Veh. Technol.*, vol. 42, no. 3, pp. 294–302, Aug. 1993.
[34] P. K. Ho, J. K. Cavers, and J. L. Varaldi, "The effects of constellation density on trellis-coded modulation in fading channels," *IEEE Trans. Veh. Technol.*, vol. 42, no. 3, pp. 318–326, Aug. 1993.
[35] J. K. Cavers and J. Varaldi, "Cochannel interference and pilot symbol assisted modulation," *IEEE Trans. Veh. Technol.*, vol. 42, no. 4, pp. 407–414, Nov. 1993.
[36] W. T. Webb and L. Hanzo, *Modern quadrature amplitude modulation: Principles and applications for wireless communications.* New York: IEEE Press–Pentech Press, 1994.
[37] R. V. Cox, J. Hagenauer, N. Seshadri, and C. E. W. Sundberg, "Subband speech coding and matched convolutional channel coding for mobile radio channels," *IEEE Trans. Signal Processing.*, vol. 39, no. 8, pp. 1717–1731, Aug. 1991.
[38] H. Shi, P. Ho, and V. Cuperman, "A combined CELP/Reed-Solomon codec for mobile radio applications," in *Proc. IEEE VTC'92,* Denver, CO, May 10–13, 1992, pp. 187–191.
[39] E. Biglieri and M. Luise, "Coded modulation and bandwidth-efficient transmission," in *Proc. Fifth Tirrenia Int. Workshop,* Sept. 8–12, 1991, Elsevier, The Netherlands, 1992.
[40] *IEEE Commun. Mag.*, vol. 29, no. 12, Dec. 1991.
[41] R. Stedman, H. Gharavi, L Hanzo, and R. Steele, "Transmission of subbband-coded images via mobile channels," *IEEE Trans. Circuits Syst. Video Technol.*, vol. 3, no. 1, pp. 15–27, Feb. 1993.
[42] M. Frullone, G. Riva, P. Grazioso, and C. Carciofi, "Investigation on dynamic channel allocation strategies suitable for PRMA schemes," in *1993 IEEE Int. Symp. Circuits Syst.*, Chicago, May 1993, pp. 2216–2219.
[43] M. Frullone, G. Falciasecca, P. Grazioso, G. Riva, and A. M. Serra, "On the performance of packet reservation multiple access with fixed and dynamic channel allocation," *IEEE Trans. Veh. Technol.*, vol. 42. no. 1, pp. 78–86, Feb. 1993.
[44] L. Hanzo, R. Salami, R. Steele, and P. M. Fortune, "Transmission of digitally encoded speech at 1.2 Kbaud for PCN," *IEE Proc.-I,* vol. 139, no. 4, pp. 437–447, 1992.
[45] L. Hanzo, J. C. S. Cheung, and R. Steele, "PRMA efficiency in adaptive transceivers," *IEE Electron. Lett.*, vol. 29, no. 8, pp. 697–698, Apr. 1993.
[46] A. S. Wright and W. G. Durtler, "Experimental performance of an adaptive digital linearized power amplifier," *IEEE Trans. Veh. Technol.*, vol. 41, no. 4, pp. 395–400, Nov. 1992.

[47] M. Faulkner and T. Mattson, "Spectral sensitivity of power amplifiers to quadrature modulator misalignment," *IEEE Trans. Veh. Technol.*, vol. 41, no. 4, pp. 516–525, Nov. 1992
[48] J. K. Cavers, "An analysis of pilot symbol assisted modulation for rayleigh fading channels," *IEEE Trans. Veh. Technol*, vol. 40, no. 4, pp. 686–693, Nov. 1991.
[49] A. Bateman and J. P. McGeehan, "Feedforward transparent tone in band for rapid fading protection in multipath fading," in *IEE Int. Conf. Commun.*, vol. 68, 1986, pp. 9–13.
[50] A. Bateman, "Feedforward transparent tone in band: Its implementation and applications," *IEEE Trans. Veh. Tech.*, vol. 39, no. 3, pp. 235–243, Aug. 1990.
[51] J. K. Cavers, "The performance of phase locked transparent tone in band with symmetric phase detection," *IEEE Trans. Commun.*, vol. 39, no. 9, pp. 1389–1399, Sept. 1991.
[52] L. Hanzo and J. Stefanov, "The Pan-European digital cellular mobile radio system—Known as GSM," in *Mobile Radio Communications*, R. Steele, Ed. London: Pentech Press, 1992, ch. 8, pp. 677–773.
[53] D. J. Goodman and S. X. Wei, "Efficiency of packet reservation multiple access," *IEEE Trans. Veh. Technol.*, vol. 40, no. 1, pp. 170–176, Feb. 1991.
[54] J. C. S. Cheung, L. Hanzo, W. T. Webb, and R. Steele, "Effects of packet reservation multiple access on objective speech quality," *Electron. Lett.*, vol. 29, no. 2, pp. 152–153, Jan. 1993.
[55] E. Bacs and L. Hanzo, "A simple real-time adaptive speech detector for SCPC systems," in *Proc. ICC'85*, Chicago, IL, pp. 1208–1212.
[56] M. R. Schroeder, "Reference signal for signal quality studies," *J. Acoustical Soc. America*, vol. 44, no. 6, pp. 1735–1736, 1968.

Lajos Hanzo (M'91–SM'92) graduated in electronics in 1976, and in 1983 he was received the Ph.D. degree.

During his 18-year career in telecommunications he has held various research and academic posts in Hungary, Germany, and the UK. Since 1986 he has been with the Department of Electronics and Computer Science, University of Southampton, UK, and has been a consultant to Multiple Access Communications Ltd., UK. He co-authored two books on mobile radio communications and published over eighty research papers.

Dr. Hanzo was awarded a number of distinctions. He is a member of the IEE.

Jason P. Woodard was born in Northern Ireland in 1969. He received the B.A. degree in physics from Oxford University in 1991, and the M.Sc. degree in electronics from Southampton University in 1992. He is currently working in Southampton towards the Ph.D. degree in speech coding.